Russian Journal of Earth Sciences, Vol. 23, ES2006
https://doi.org/10.2205/2023ES000839

COVID-19 Pandemic Course 2020–2022: Description by Methods of Mathematical Statistics and Discrete Mathematical Analysis

A. D. Gvishiani[1,2], A. A. Odintsova[1], E. A. Rovenskaya[3,4], G. S. Boyarshinov[1,5], I. O. Belov[1], and M. N. Dobrovolsky[*1]

[1]*Geophysical center of RAS, Moscow, Russia*
[2]*Schmidt Institute of Physics of the Earth of RAS, Moscow, Russia*
[3]*International Institute for Applied Systems Analysis, Laxenburg, Austria*
[4]*Faculty of Computational Mathematics and Cybernetics, Lomonosov Moscow State University, Moscow, Russia*
[5]*V. A. Trapeznikov Institute of Control Sciences of RAS, Moscow, Russia*

Received 22 March 2023; accepted 29 May 2023; published 31 May 2023.

The paper describes the course of the COVID-19 pandemic using a combination of mathematical statistics and discrete mathematical analysis (DMA) methods. The method of regression derivatives and FCARS algorithm as components of DMA will be for the first time tested outside of geophysics problems. The algorithm is applied to time series of the number of new cases of COVID-19 infections per day for some regions of Russia and the Republic of Austria. This allowed to assess the nature and anomalies of pandemic spread as well as restrictive measures and decisions taken in terms of the administration of countries and territories. It was shown that these methods can be used to identify time intervals of change in the nature of the incidence rate and areas with the most severe course of the epidemic. This made it possible to identify the most significant restrictive measures that allowed to reduce the growth of the disease.

Keywords: COVID-19, DMA, statistics, data analysis

Citation: Gvishiani, A. D., A. A. Odintsova, E. A. Rovenskaya, G. S. Boyarshinov, I. O. Belov, and M. N. Dobrovolsky (2023), COVID-19 pandemic course 2020–2022: description by methods of mathematical statistics and discrete mathematical analysis, *Russian Journal of Earth Sciences*, Vol. 23, ES2006, doi: 10.2205/2023ES000839.

1 Introduction

The new coronavirus pandemic COVID-19 infection that began in December 2019 [*Huang et al.*, 2020] has become an unprecedented global challenge of the 21st century for science and humanity as a whole. The fight against the pandemic has posed many serious challenges that require systemic efforts to address them.

These tasks go far beyond the scope of purely medical issues. Their solution requires systematic and analytical integration of methods of various scientific disciplines. Combining the efforts of medical researchers with the projects of scientists from allied sciences (biology, physiology, chemistry, etc.) can make a significant contribution in the future to the study of the patterns of pandemic development, including the description of the nature of its spread. A particularly important role in such a multidisciplinary approach is played by data analysis [*Odintsova et al.*, 2020; *Soloviev et al.*, 2016] and system-analytical mathematical constructs (methods) that allow the integration of the achievements of various disciplines [*Gvishiani*, 2019].

Correspondence to:
*M. N. Dobrovolsky, m.dobrovolsky@gcras.ru

The article is devoted to some results of applying a set of mathematical methods to describe the course of the COVID-19 pandemic. The set includes both well-known, generally accepted methods of mathematical statistics and innovative algorithms of discrete mathematical analysis (DMA) [*Agayan et al.*, 2018; *Dzeboev et al.*, 2022].

The paper analyzes data describing the spread of coronavirus since the first confirmed cases of infection in a number of subjects of the Russian Federation and the Republic of Austria. The choice of subjects for comparison is not accidental and is defined by the international joint project of Geophysical Center of the Russian Academy of Sciences (GC RAS) with the International Institute for Applied Systems Analysis (IIASA), located in Laxenburg, Austria.

The availability of statistical information allows pandemic events to be presented as a time series. The study of the properties of these time series, in turn, makes it possible to draw conclusions about the nature and anomalies of the pandemic spread, the restrictive measures taken and the decisions made in terms of administration of countries and territories.

2 Input data

Initially, sources of information that met the objectives of the project were searched. One of the criteria for the use of data sets was the availability of detailed records on the subjects of the Russian Federation and European countries in comparable temporal and spatial scales.

The selected data can be divided into two (I and II) groups according to the type of information to be collected:

1. *Epidemiological parameters of the course of the pandemic*: the number of infections, recoveries, and deaths. The data sources used for the first group were:
   (a) Yandex dataset [*Yandex DataLens*, 2023], daily aggregating the above data from the site [https://xn--80aesfpebagmfblc0a.xn--p1ai/] in the time range from 12.03.2020 to 13.01.2023 for all subjects of the Russian Federation, including federal cities: Moscow, St. Petersburg, and Sevastopol;
   (b) Johns Hopkins University (JHU) Center for Systems Science and Engineering COVID-19 Data Repository [*GitHub*, 2023], daily aggregating data in the time range from 22.01.2020 to the current day for the countries of the world;
2. *Chronology of restrictive measures taken in European countries to contain the spread of the pandemic*. The source here was a data set of the World Health Organization (WHO) [*World Health Organization*, 2019], where as of November 1, 2022 1317 records on the subjects of the Russian Federation (including 213 records on Moscow, 91 records on St. Petersburg, 17 records on Kaliningrad Oblast, 2 records on Sevastopol and the Crimea) and 46,174 records on European countries (including 1145 records on Austrian Rep.) were collected.

For further references to data sources in the text of the article, the abbreviated names of their aggregators will be used: YAND, JHU, and WHO.

The data of the preliminary results of the All-Russian Population Census of 01.10.2021 were used for the number of population in the subjects of the Russian Federation [*Rossiyskaya Gazeta*, 2022]. For a comparative assessment of the dynamics of mortality the data of the State Automobile Inspectorate [*GIBDD*, 2023] were used.

The work assesses the course of the pandemic in five subjects of the Russian Federation: Moscow (Figure 1), St. Petersburg (Figure 2), Sevastopol (Figure 3), Crimea (Figure 4), Kaliningrad Region (Figure 5) and the Republic of Austria (Figure 6). In the figures corresponding to the regions, graphic visualizations of the time series of the number of new COVID-19 infections (section a), recoveries (section b) and deaths (section c) per day in the time range from 12.03.2020 to 01.11.2022 (965 days) are shown. Also for each of the selected subjects of the Russian Federation, a time series of the total number of infections per date, normalized per 100,000 population of the subject (section d), was calculated and visualized. It should be noted that the calculation of a similar time series for the Austrian Rep. was not possible, because the JHU does not record the values of the number of new cases of recoveries since 05.08.2021.

Total numbers of COVID-19 infections, recoveries, and per countries and subjects of the Russian Federation are visualized via the system of interactive geospatial 3D visualizations virtual hyperglobe "ORBUS WEB 1.0 COVID-19" [*ORBUS Web*, 2019]. The ease of use of digital globes and their capacity to display spatial information make them a powerful tool to communicate and make data accessible to a range of users including decision-makers, researchers, and the general public [*Aurambout et al.*, 2008].

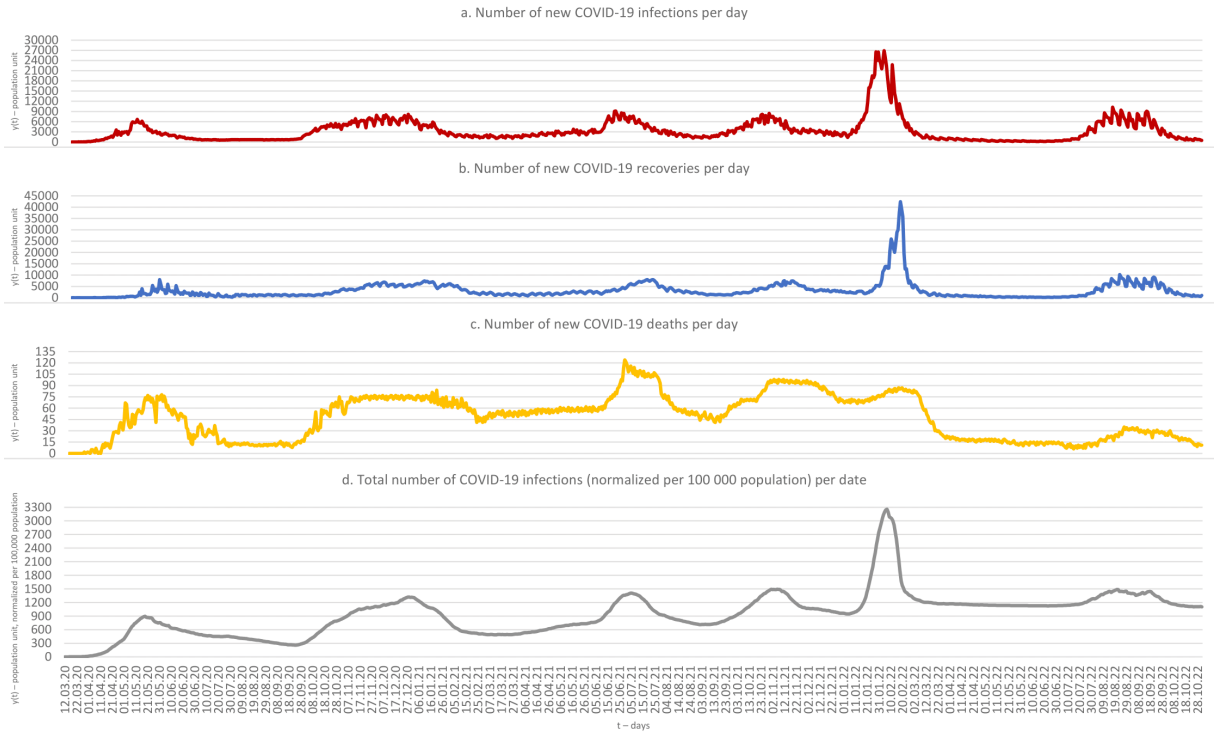

Figure 1: Series of the number of new COVID-19 cases (a) infections, (b) recoveries, (c) deaths per day, and (d) the total number of infections per day, normalized per 100,000 population for Moscow from 12.03.2020 to 01.11.2022.

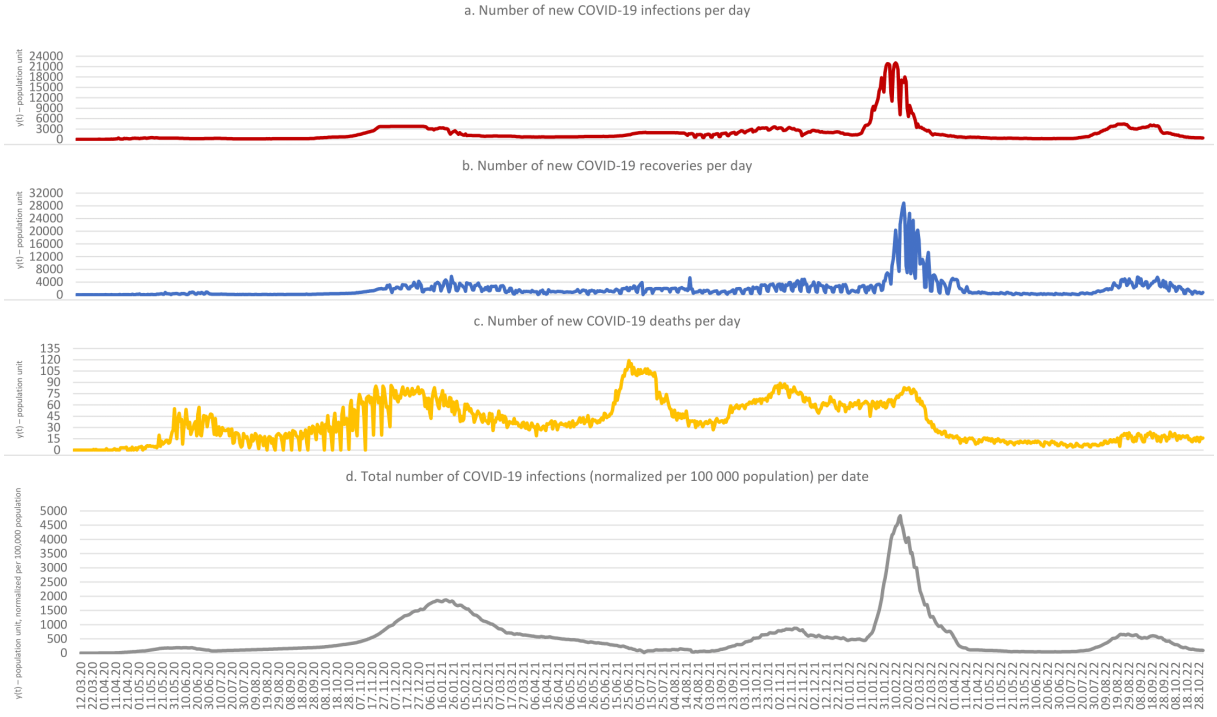

Figure 2: Series of the number of new COVID-19 cases (a) infections, (b) recoveries, (c) deaths per day, and (d) the total number of infections per day, normalized per 100,000 population for St. Petersburg from 12.03.2020 to 01.11.2022.

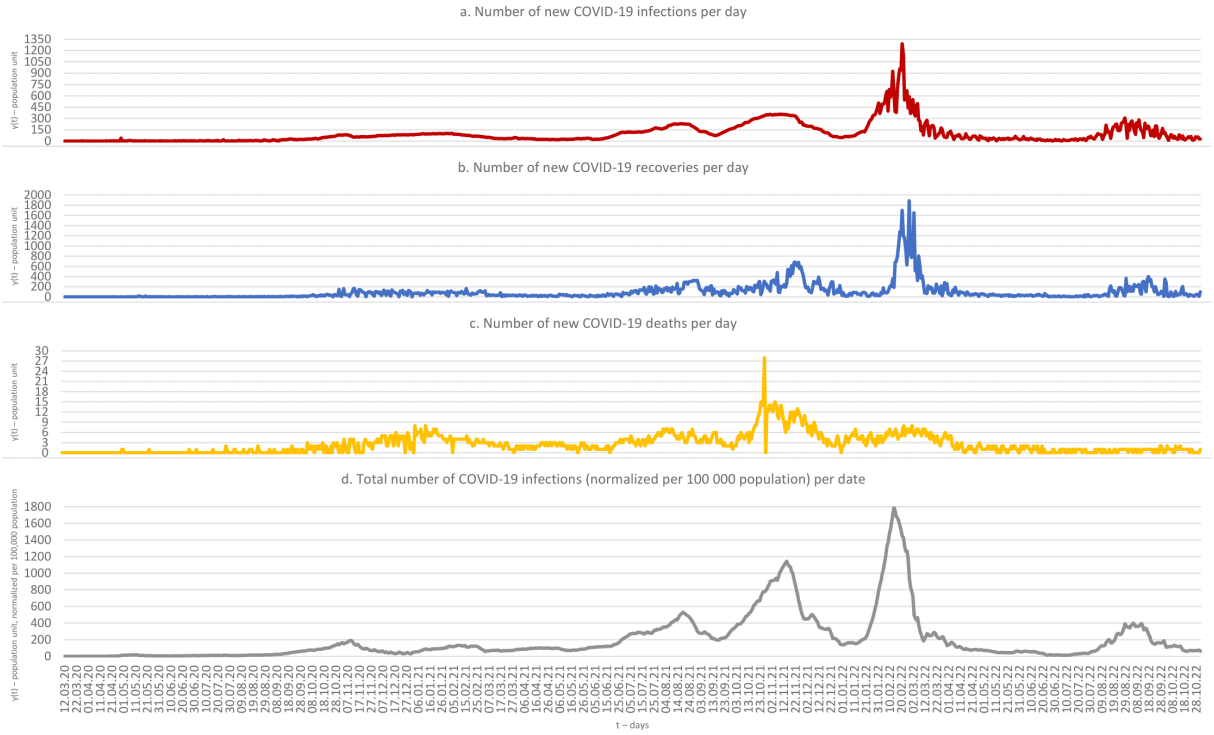

Figure 3: Series of the number of new COVID-19 cases (a) infections, (b) recoveries, (c) deaths per day, and (d) the total number of infections per day, normalized per 100,000 population for Sevastopol from 12.03.2020 to 01.11.2022.

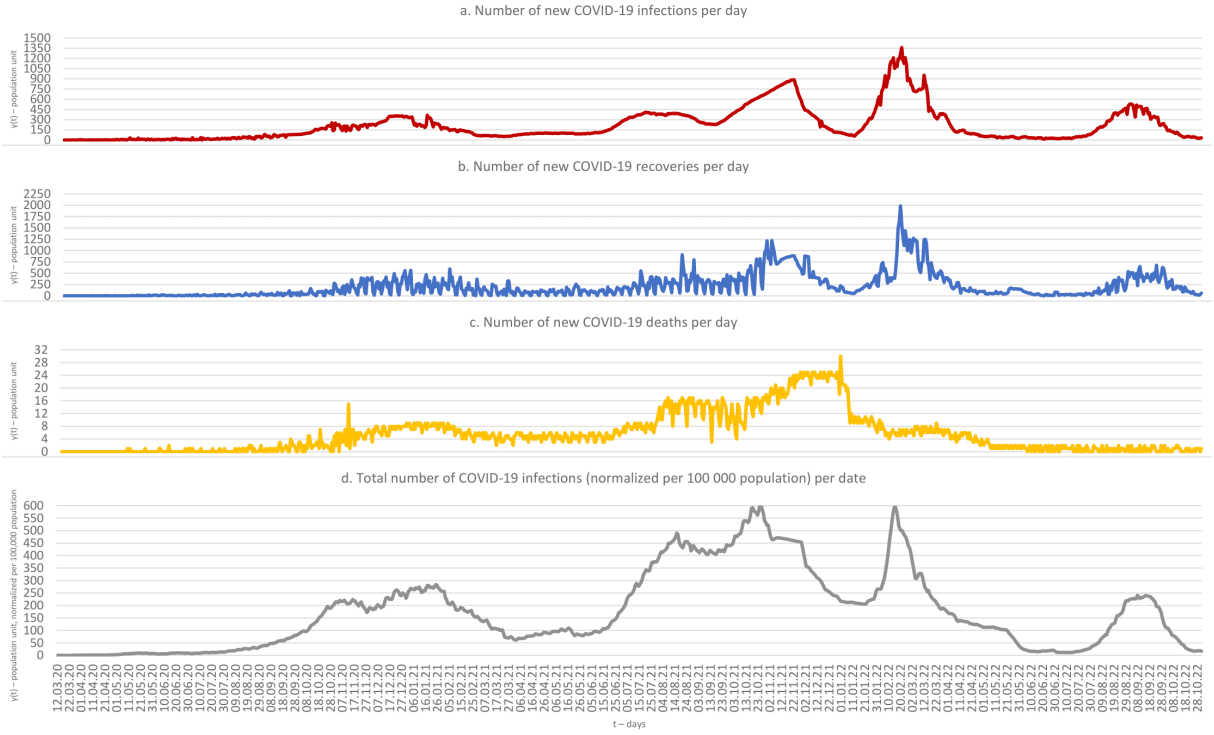

Figure 4: Series of the number of new COVID-19 cases (a) infections, (b) recoveries, (c) deaths per day, and (d) the total number of infections per day, normalized per 100,000 population for the Republic of Crimea from 12.03.2020 to 01.11.2022.

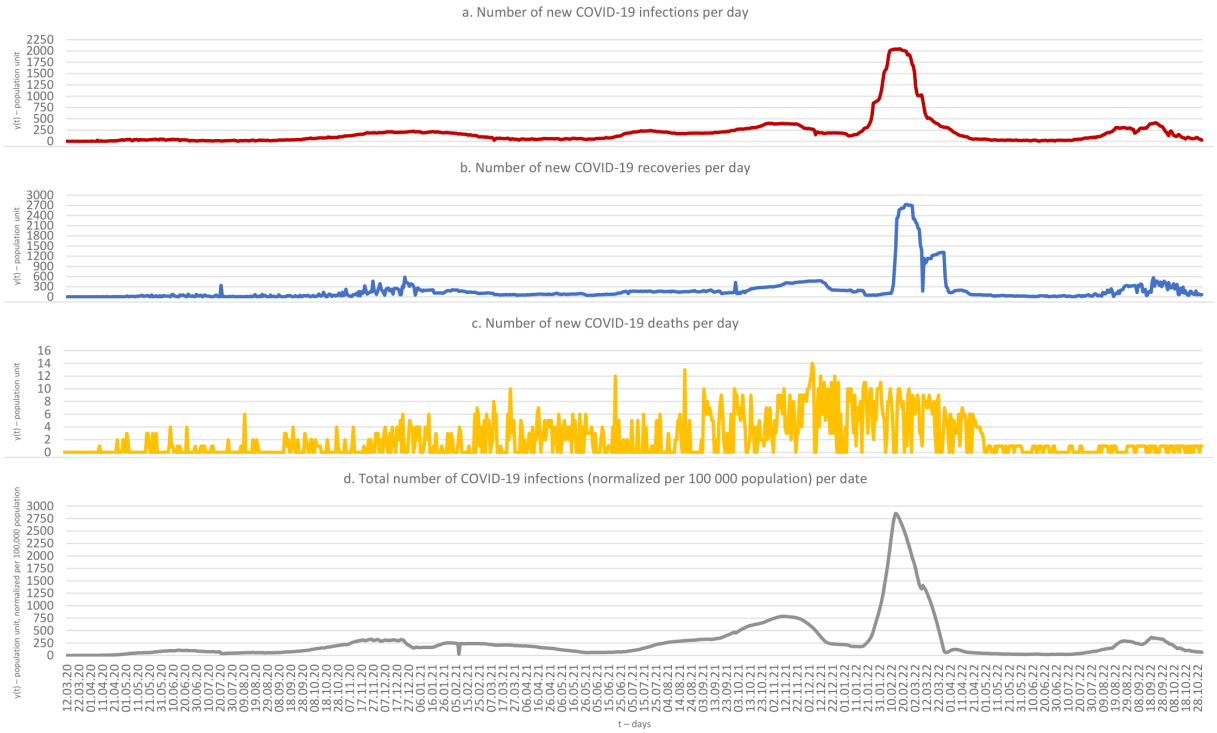

Figure 5: Series of the number of new COVID-19 cases (a) infections, (b) recoveries, (c) deaths per day, and (d) the total number of infections per day, normalized per 100,000 population for Kaliningrad oblast from 12.03.2020 to 01.11.2022.

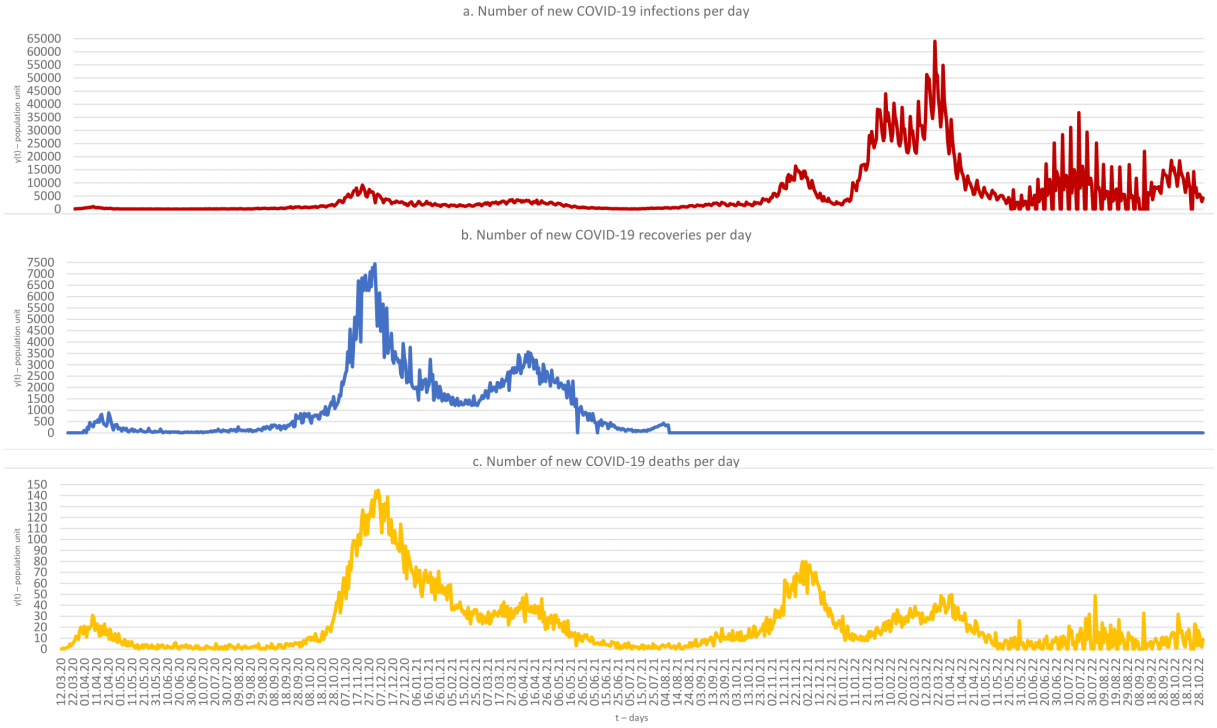

Figure 6: Series of the number of new COVID-19 cases (a) infections, (b) recoveries, (c) deaths per day Austrian Rep. from 12.03.2020 to 01.11.2022. (JHU does not record values for the number of new cases of recoveries since 5.08.2021).

3 Statistical analysis of the COVID-19 pandemic course

3.1 Correlation analysis of time series

To search for patterns in the course of the COVID-19 pandemic in the six regions in question the cross-correlations of the time series presented in Figure 1–6 were analyzed.

Table 1 shows the values of the correlation coefficients $k^n_{i,j}$ between pairs of time series i and j (1 – the number of new infections per day, 2 – the number of new cases of recoveries per day, 3 – the number of new deaths per day, 4 – the total number of infected as of the date) in the region n (1 – Moscow, 2 – St. Petersburg, 3 – Sevastopol, 4 – Crimea Rep., 5 – Kaliningrad region); index n determines the subtable number, indexes i and j – row and column of the cell.

Note that in the studied subjects of the Russian Federation, there is often a pronounced positive correlation between the time series of the number of new cases of infections and recoveries per day ($k^n_{2,1}$): **which indicates the transitivity of the processes** [*Saxena et al.*, 2022]. Moreover, in general, the smaller the population of a constituent entity of the Russian Federation, the greater $k^n_{2,1}$.

Table 2 shows the values of the correlation coefficients $r^n_{i,j}$ between time series n (1 – the number of new infections per day, 2 – the number of new cases of recoveries per day, 3 – the number of new deaths per day, 4 – the total number of infected as of the date), characterizing a pair of regions i and j (1 – Moscow, 2 – St. Petersburg, 3 – Sevastopol, 4 – Crimea Rep., 5 – Kaliningrad region, 6 – Austrian Rep.); index n determines the subtable number, indexes i and j – row and column of the cell.

Note that there is a pronounced positive correlation between the time series of the number of new infections, recoveries, and deaths per day for many pairs of studied regions of the Russian Federation. **This illustrates the similarity in the dynamics of the pandemic in these constituent regions of the Russian Federation**. The highest correlation occurs in pairs Moscow – St. Petersburg ($r^n_{2,1}$) and Sevastopol – Crimea Rep. ($r^n_{4,3}$). The similarity of dynamics in the first pair is naturally explained by the territorial and transport proximity of the cities. In the second pair, the similarity of dynamics is determined by the geographical proximity of the regions on the same peninsula. The subjects of both pairs are also characterized by high cyclic traffic of transport links.

Table 1: Values of correlation coefficients $k^n_{i,j}$. Index n determines the subtable number, indexes i and j – row and column of the cell

Moscow	Infections per day	Recoveries per day	Deaths per day	Total number of infected
Infections per day	1			
Recoveries per day	0.562938977	1		
Deaths per day	0.488429399	0.485220584	1	
Total number of infected	0.682719214	0.634364722	0.38332898	1
St. Petersburg	**Infections per day**	**Recoveries per day**	**Deaths per day**	**Total number of infected**
Infections per day	1			
Recoveries per day	0.64016228	1		
Deaths per day	0.406394508	0.365338097	1	
Total number of infected	0.811082998	0.751588059	0.460550596	1
Sevastopol	**Infections per day**	**Recoveries per day**	**Deaths per day**	**Total number of infected**
Infections per day	1			
Recoveries per day	0.738854362	1		
Deaths per day	0.59671243	0.493865275	1	
Total number of infected	0.921670552	0.679162114	0.647886886	1
Crimea Rep.	**Infections per day**	**Recoveries per day**	**Deaths per day**	**Total number of infected**
Infections per day	1			
Recoveries per day	0.846445438	1		
Deaths per day	0.488566348	0.500071265	1	
Total number of infected	0.82489322	0.706265408	0.751662862	1
Kaliningrad region	**Infections per day**	**Recoveries per day**	**Deaths per day**	**Total number of infected**
Infections per day	1			
Recoveries per day	0.756660355	1		
Deaths per day	0.38710515	0.352082048	1	
Total number of infected	0.956961024	0.788041885	0.428597162	1

Table 2: Values of correlation coefficients $r^n_{i,j}$. Index n determines the subtable number, indexes i and j – row and column of the cell

Infections per day	Moscow	St. Petersburg	Sevastopol	Crimea Rep.	Kaliningrad region	Austrian Rep.
Moscow	1					
St. Petersburg	0.802667149	1				
Sevastopol	0.505833063	0.746333688	1			
Crimea Rep.	0.509039416	0.697500346	0.908407717	1		
Kaliningrad region	0.529599673	0.838192337	0.872443674	0.822683758	1	
Austrian Rep.	0.333878184	0.536365647	0.508738171	0.519882201	0.638959037	1

Recoveries per day	Moscow	St. Petersburg	Sevastopol	Crimea Rep.	Kaliningrad region
Moscow	1				
St. Petersburg	0.73597217	1			
Sevastopol	0.480899421	0.688414144	1		
Crimea Rep.	0.542716917	0.69422487	0.770550067	1	
Kaliningrad region	0.485166577	0.777123339	0.807214694	0.736531848	1

Deaths per day	Moscow	St. Petersburg	Sevastopol	Crimea Rep.	Kaliningrad region	Austrian Rep.
Moscow	1					
St. Petersburg	0.865100603	1				
Sevastopol	0.625697757	0.632540937	1			
Crimea Rep.	0.645069915	0.622804763	0.72713008	1		
Kaliningrad region	0.37566987	0.35446118	0.451005364	0.503062554	1	
Austrian Rep.	0.399861613	0.402205622	0.33021934	0.31581971	0.173683442	1

Total number of infected	Moscow	St. Petersburg	Sevastopol	Crimea Rep.	Kaliningrad region
Moscow	1				
St. Petersburg	0.587355349	1			
Sevastopol	0.631741532	0.664188968	1		
Crimea Rep.	0.464082131	0.457751158	0.765739263	1	
Kaliningrad region	0.575901095	0.831521306	0.872163148	0.634349094	1

Correlation between the time series of the number of new infections and deaths per day between any subject of the Russian Federation and Austrian Rep. ($r^1_{6,n}$ and $r^3_{6,n}$ respectively) is weakly pronounced, which suggests that the course of the pandemic is not similar in the compared regions.

3.2 Recognition of key restrictive measures using regression derivatives

This part focuses on the identification of restrictive measures from WHO records that influenced the reduction of new COVID-19 infections per day in three of the regions considered above: Moscow, St. Petersburg and the Republic of Austria. The reason for the restriction to the three regions is the availability of sufficient WHO records corresponding to the region – a record of measures used in selected regions to contain the spread of the pandemic.

As a source of data on the number of new infections per day for Moscow and St. Petersburg, YAND was used; for the Republic of Austria, JHU was used. It should be noted that there are meaningful duplications of the same restrictive measures among WHO records for the regions surveyed. Such duplications were preliminarily deleted. Thus, 193 unique events out of 213 available were selected for Moscow, 87 out of 91 for St. Petersburg, and 1009 out of 1145 for the Republic of Austria.

At the first stage of the analysis, the regression derivative [*Agayan et al.*, 2018, 2019a,b, 2021], which is a transfer of the classical concept of differentiation to the discrete case, is calculated for the time series from YAND. One of the free parameters of this operation governs the choice of the scale of "overview" of the discrete time series under study [*Agayan et al.*, 2021; *Gvishiani et al.*, 2008].

The regression derivative is defined as the angular coefficient of the regression tangent (linear regression) plotted at a given point in time t to the discrete time series plot $y(t)$, weighted using a proximity measure δ_t. The latter is one of the ba-

sic concepts within the DMA [*Gvishiani et al.*, 2008; *Kolmogorov and Fomin*, 2004].

To calculate the regression derivative, the global or local proximity measures for a discrete time series y, defined on the area of definition T, are used. The global proximity measure is given by the formula:

$$\delta_t(t') = \delta_t(r,p)(t') = \left(1 - \frac{|t'-t|}{\max(\max T - t,\ t - \min T) + r}\right)^p, \quad t, t' \in T.$$

The local proximity measure is given by the formula:

$$\delta_t(t') = \delta_t(r,p)(t') = \begin{cases} \left(1 - \frac{|t'-t|}{r}\right)^p, & |t'-t| \le r, \\ 0, & |t'-t| > r. \end{cases}, \quad t, t' \in T$$

where r is the radius of localization, and the free parameter p will be called the regression derivative parameter. It sets the scale of the time series y overview.

The proximity measure allows to determine the regression tangent $R_{y,t}(t') = a_t t' + b_t$ to the sequence y at the point t as a linear regression based on a weighted plot $\Gamma_y(\delta_t) = \{(t', y(t'), \delta_t(t'))\}$.

Finally, the regression derivative $y'(t)$ at the point t is called the angular coefficient a_t of regression tangent $R_{y,t}$ [*Agayan et al.*, 2021; *Gvishiani et al.*, 2008].

Next, the regression derivatives of the original time series of the number of new infections per day were calculated:

1. for Moscow was considered a time interval from 12.03.2020 to 01.11.2022, the parameter of the regression derivative $p = 4$, localization radius $r = 14$ (Figure 7). On the graph there is also regression smoothing R_y of the original time series, which represents the values of the regression tangents $R_{y,t}(t)$ at each point t;

2. for St. Petersburg the same interval of time series from 12.03.2020 to 01.11.2022 was taken, the parameter of the regression derivative $p = 10$, localization radius $r = 14$ (Figure 8). The choice here of the parameter p, which is 2.5 times larger than for Moscow, is explained by the smaller number of restriction measures taken for this subject and by an attempt to isolate more detailed disturbances on a less rugged graph;

3. for the Austrian Rep. the time series interval from 22.01.2020 to 10.11.2022 was considered, the parameter of the regression derivative $p = 4$, localization radius $r = 14$ (Figure 9).

Then to the regression derivative of the time series $f(x)$ discrete convolution [*Kolmogorov and Fomin*, 2004] was applied with a convolution kernel $g(-x) = (-1, 0, 1)$:

$$(f * g)(x) = \sum_{t=-\infty}^{\infty} f(t)\ g(x-t).$$

Peaks of the convolution function $(f * g)(x)$ indicate the beginning of the decrease in the number of new infections per day. As an example, let us compare the peaks of the convolution function and the smoothed time series of the number of new cases per day for Moscow (Figure 10).

In the next step, the function $(f * g)(x)$ is divided by level α, to select the days of the "tops" of the peaks (Figure 11) [*Gvishiani et al.*, 2008].

To find the level α for the city of Moscow we take the parameter of fuzzy comparison $\beta = 0.035$, for St. Petersburg – $\beta = 0.005$, and for the Republic of Austria – $\beta = 0.023$. Less stringent level α for St. Petersburg is also associated with an attempt to isolate less pronounced fluctuations in the time series.

In the last step, after identifying the days when the number of new infections per day began to decrease, from the total number of days is subtracted δ, equal to the number of days required for the coronavirus to incubate. Within the framework of the study, the authors accepted the duration of the incubation period equal to 7 days, as well as a window ±5 days [*Rospotrebnadzor*, 2023]. The dates obtained are then compared with the dates of relevant events on the list of restrictive measures from WHO to obtain the final result.

Thus, for Moscow in the period from 12.03.2020 to 01.11.2022, which is 965 days, 254 "peak" days were identified in terms of decreasing derivative, when the number of new cases of infections per day begins to decrease (Figure 12). There are 193 unique events in the WHO records over the study period, of which 127 were identified as affecting the decrease in the number of new infections per day.

Based on the recognized events and their analysis (Table 3), we note the following key restrictive measures implemented by the Moscow City Government as effective, some of which are shown in Figure 12:

1. electronic QR-code pass system for travel in personal and public transport around the city (15.04.2020);

2. tracking the movements of people with COVID-19 symptoms using geolocation data, and self-isolating them at home (21.04.2020);

3. 30% of employees transferred by employers to remote work (22.09.2020);

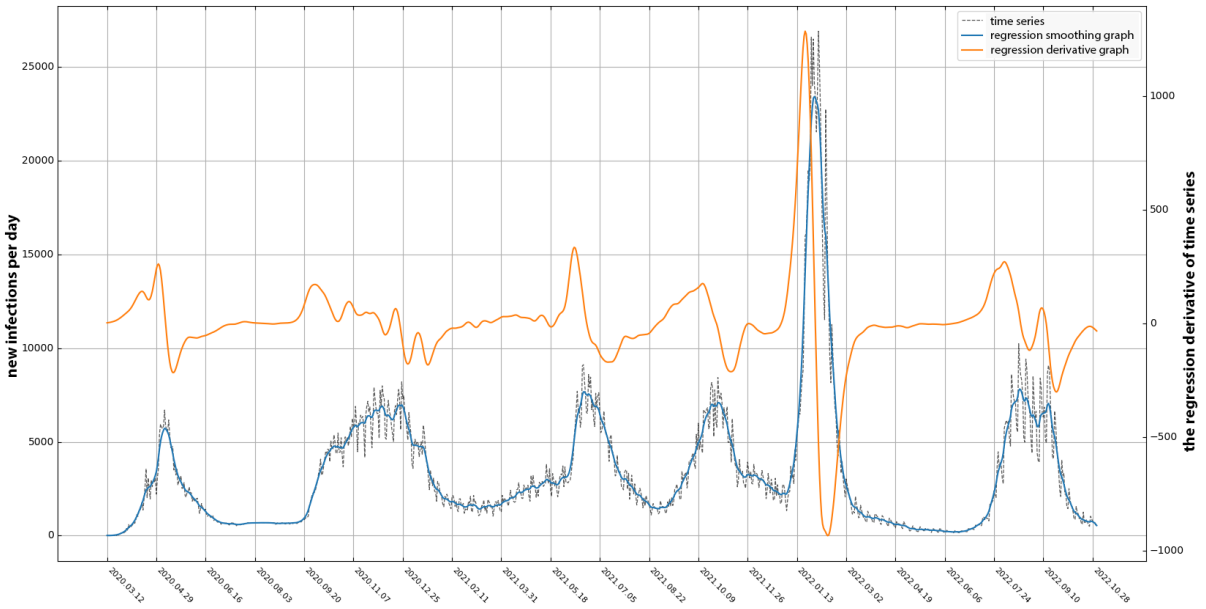

Figure 7: The time series graph of the number of new infections per day for Moscow from 12.03.2020 to 01.11.2022 from YAND is shown in black; its regression smoothing graph is shown in blue; the graph of its regression derivative with the parameter $p = 4$ in orange.

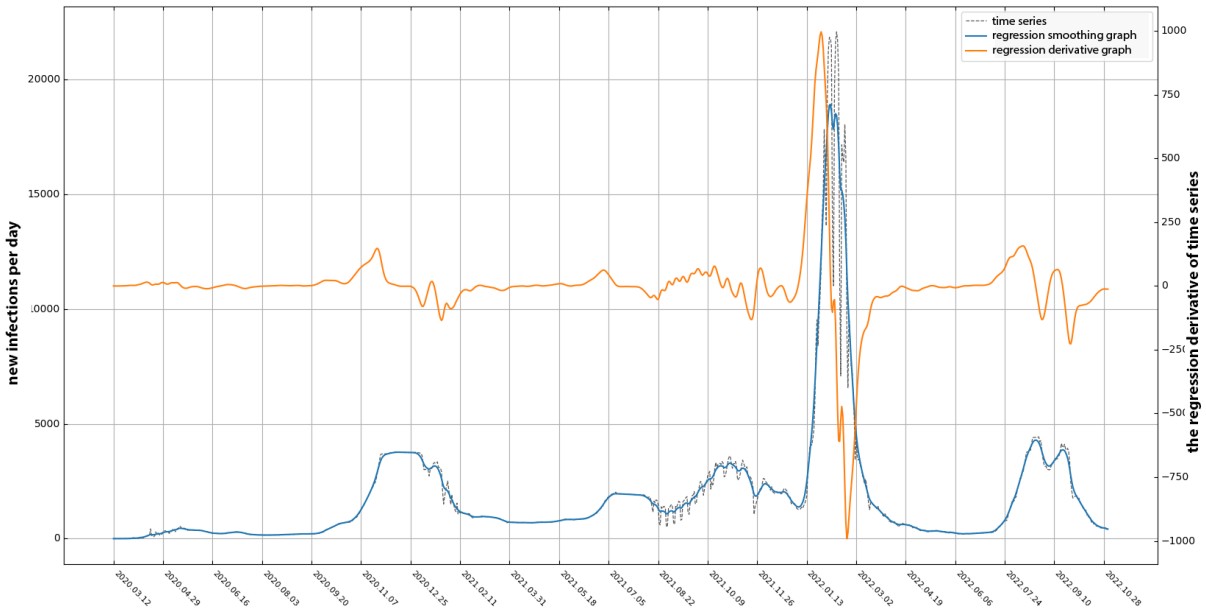

Figure 8: The time series graph of the number of new infections per day for St. Petersburg from 12.03.2020 to 01.11.2022 from YAND is shown in black; its regression smoothing graph is shown in blue; the graph of its regression derivative with parameter $p = 10$ in orange.

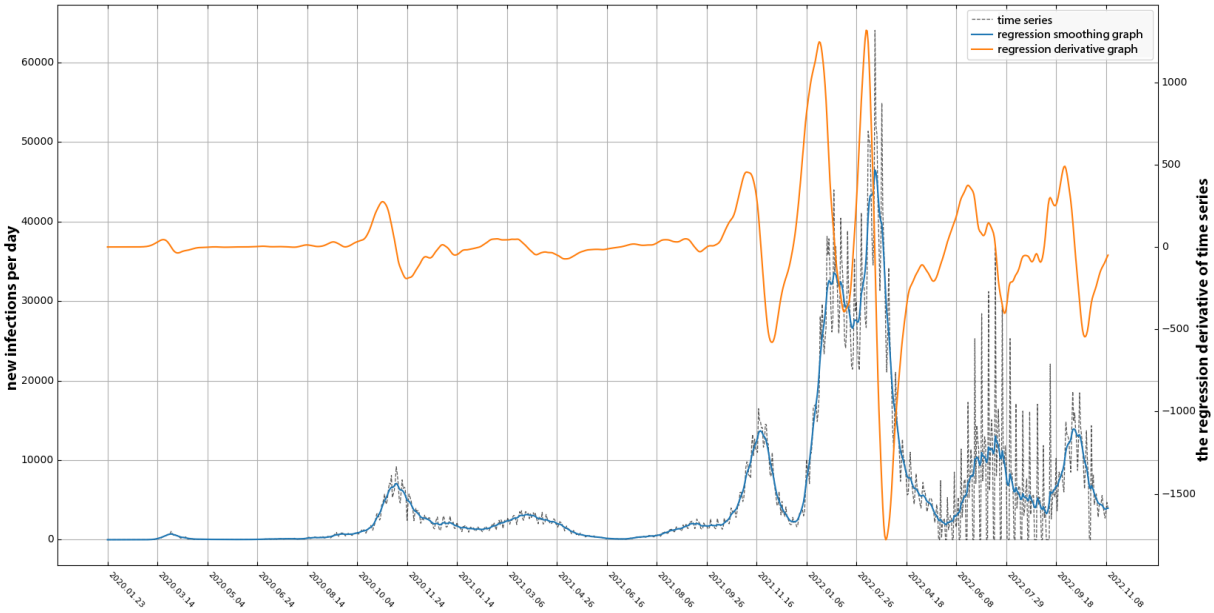

Figure 9: The time series graph of the number of new infections per day for Austria Rep. from 22.01.2020 to 10.11.2022 is shown in black; its regression smoothing graph is shown in blue; its regression derivative graph with parameter $p = 4$ in orange.

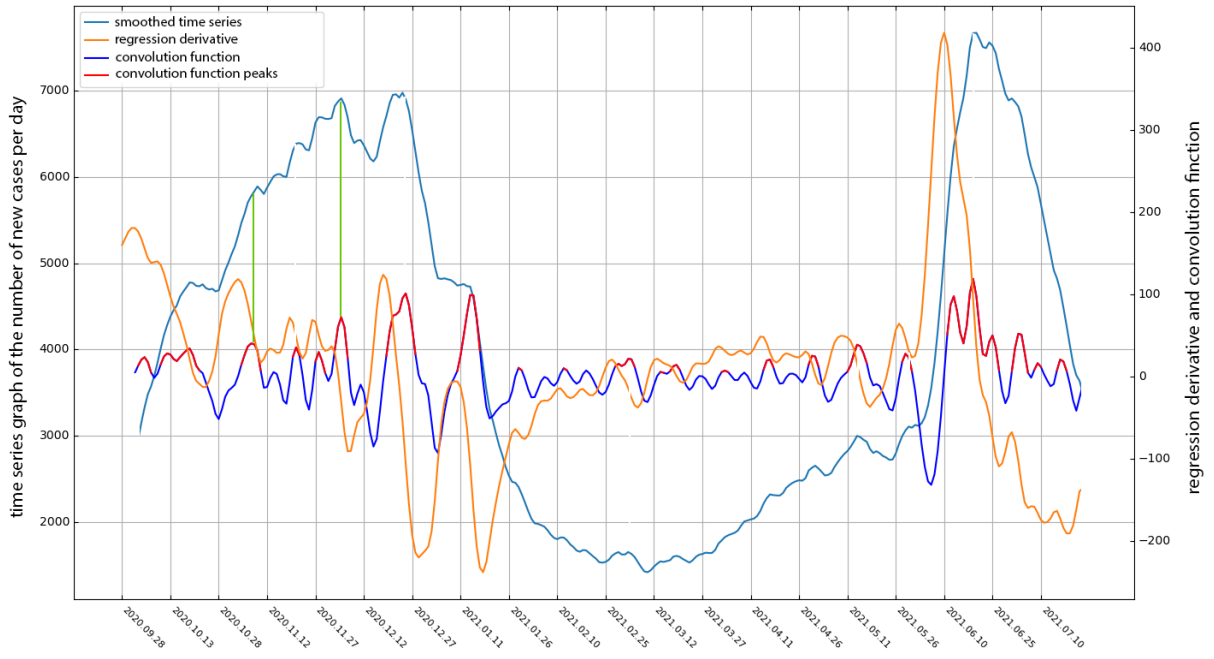

Figure 10: The smoothed time series graph of the number of new cases per day for Moscow from 28.09.2020 to 28.07.2021 from JHU is shown in blue; the graph of its regression derivative is shown in orange; the graph of its convolution function with a negative trend kernel is shown in blue. The local maxima of the convolution function indicate where the number of new infections per day began to decline (these locations are marked by green vertical lines in the graph).

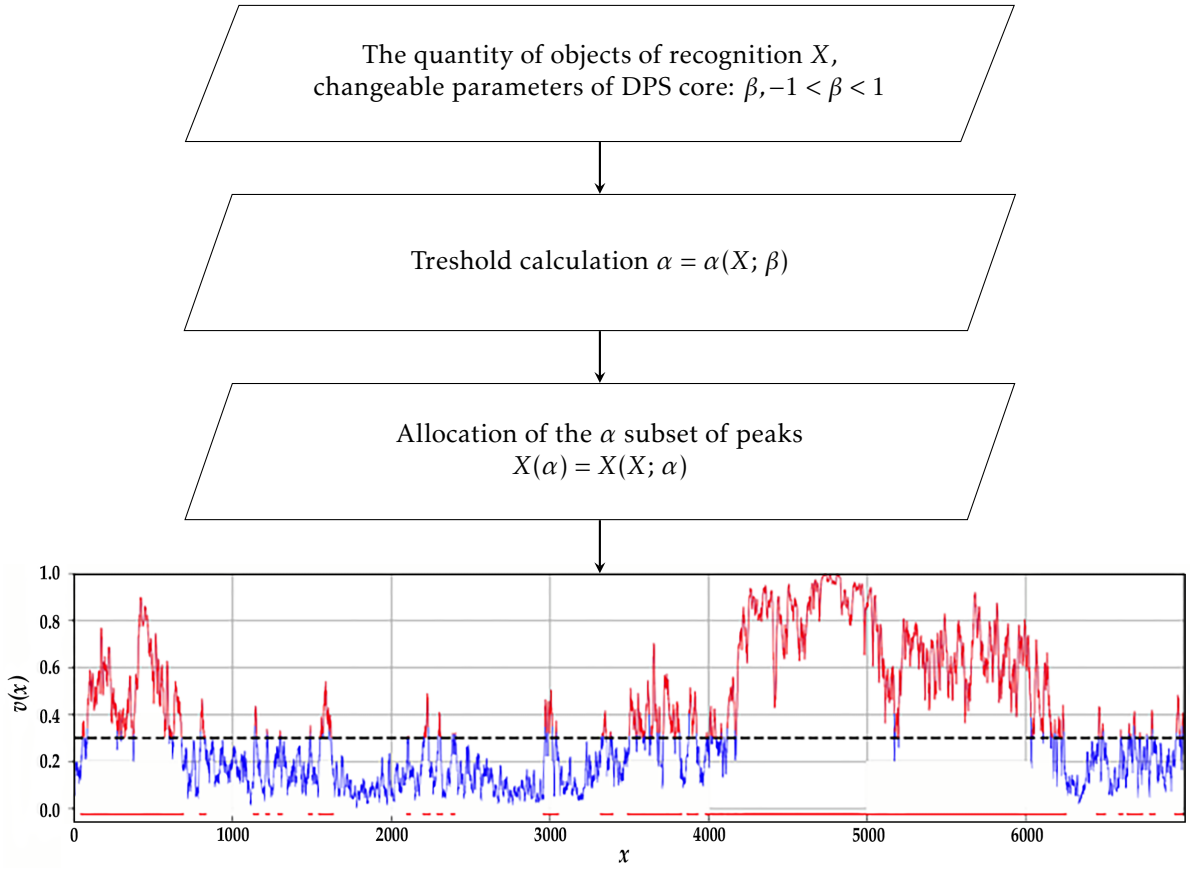

Figure 11: Block diagram of the classic level α search on the set, using the fuzzy comparison parameter $\beta \in [-1, 1]$. Anomalies identified by level are shown in red. The dotted line indicates the set threshold $\alpha = 0.3$.

4. closure of restaurants and nightlife entertainment venues from 11:00 a.m. to 06:00 p.m. until January 15, 2021, due to an outbreak of coronavirus infection (13.11.2020);

5. tightening control over the wearing of gloves and masks in public places (09.06.2021);

6. vaccination of workers in trade, housing and utilities, sports, culture, education, health care, transport (including cabs), catering, consumer services, beauty industry, post office, and MFC (16.06.2021);

7. keeping people over 60 years of age in isolation with a recommendation to go outside in extreme cases (23.01.2022);

8. Moscow residents and guests are advised to wear protective masks in closed public places with increased congestion (12.07.2022).

For St. Petersburg in the period from 12.03.2020 to 01.11.2022, which is 965 days, 269 "peak" days were identified in terms of decreasing derivative, when the number of new cases of infections per day begins to decrease (Figure 13). There are 87 unique events in the WHO records over the study period, of which 61 were identified as affecting the decrease in the number of new infections per day.

Based on the recognized events and their analysis (see further in Table 3), the following key restrictive measures implemented by the Government of St. Petersburg were noted as effective. Some of them are shown in Figure 13:

1. self-isolation regime is declared for residents (30.03.2020);

2. extension of quarantine until May 31, 2020 and requirements to wear masks and gloves in public places (11.05.2020);

3. the activities of food courts and catering facilities in shopping malls were suspended (18.11.2020);

4. occupancy of concert halls in theaters and cinemas should not exceed 25% of the number of seats in the hall (01.12.2020);

5. prohibition of restaurants and catering establishments from 19:00 to 06:00 (25.12.2020);

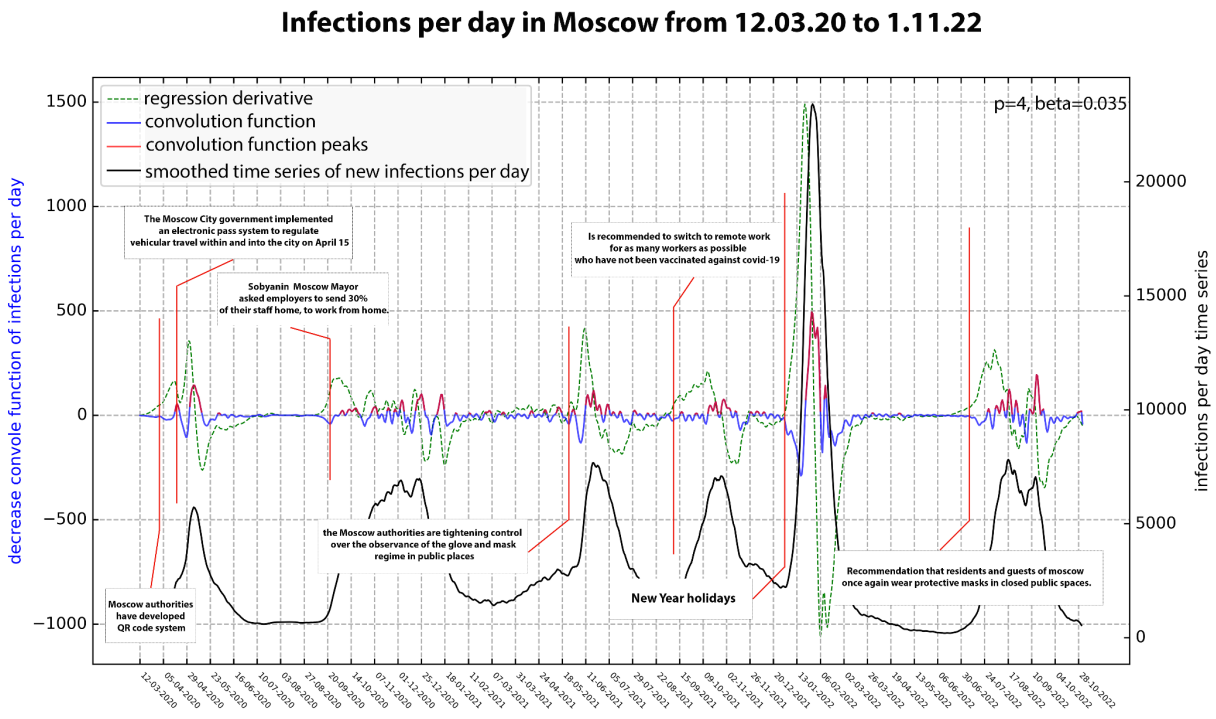

Figure 12: The smoothed time series graph of the number of new infections per day for Moscow from 12.03.2020 to 01.11.2022 from YAND is shown in black; its convolution function graph and highlighted peaks by threshold α in blue and red, respectively. The dates of introduction of the selected key restrictive measures are marked with red signposts with textual explanations.

6. lifting the ban on the operation of food courts and catering facilities, trade and services in shopping centers; among the requirements for companies is the vaccination of all employees except those who have recently contracted the disease (02.08.2021);

7. showing QR codes confirming vaccination status or a negative PCR test to visit theaters, cinemas, swimming pools and gyms until November 2021 (12.10.2021).

For the Austrian Rep. (Figure 14), 311 "peak" days in terms of decreasing derivative, when the number of new infections per day begins to decrease, were highlighted for the period from January 22, 2020, to November 10, 2022, which is 1125 days. There are 1009 unique events in the WHO records over the study period, of which 630 were identified as affecting the decrease in new infections per day.

Based on the recognized events and their analysis (see Table 3 below), the following key restrictive measures implemented by the Austrian government were noted as effective. Some of them are shown in Figure 14:

1. ban on flights from some countries where COVID-19 outbreaks have occurred, as well as a 14-day home quarantine for visitors from high-risk countries; cancellation of outdoor events with more than 500 participants and indoor events with more than 100 participants (11.03.2020);

2. providing contact information for visitors to restaurants and bars to alert them in cases where contamination has been detected; meetings are limited to a maximum of six adults indoors and twelve outdoors; mandatory wearing of masks in all common areas; testing of citizens when traveling within the country; maintaining specific rules for disinfecting spaces to prevent the spread of COVID-19 for all establishments; mandatory wearing of masks by staff (23.10.2020);

3. departure from some regions is allowed only with a negative PCR result (not older than 72 hours), with a certificate of vaccination, or after a full recovery; mandatory wearing of FF2 masks in public places and enclosed spaces (08.11.2021).

In general, the measures in the Republic of Austria are similar to those taken in Moscow and St. Petersburg, but in some cases reinforced measures were applied: the use of masks of protection

Table 3: Nominal number of key restrictive measures identified by regression derivatives and their percentage composition, based on WHO classification category affiliation, for Moscow, St. Petersburg, and Austrian Rep.

Region	Total key restrictive measures selected	Percentage breakdown, from WHO categorization (category code indicated in parentheses)									
		Wearing masks and hygiene measures (1)	Identifying and isolating cases of infection (3.1)	Measures in schools (4.1)	Offices, businesses, universities (4.2)	Meetings, Business and Services (4.3)	Protection of vulnerable groups (65+ years) (4.4)	Domestic travel (4.5)	Measures for international travel (5.7)	Use of vaccines for prevention (7.2)	Other (8)
Moscow	127	8 (6%)	8 (6%)	15 (11%)	42 (33%)	15 (11%)	11 (8%)	14 (11%)	–	9 (7%)	5 (4%)
St. Petersburg	61	2 (3%)	–	4 (6%)	28 (45%)	13 (21%)	1 (2%)	7 (11%)	–	4 (6%)	2 (3%)
Austrian Rep.	630	53 (8%)	40 (6%)	57 (9%)	100 (16%)	79 (15%)	36 (8%)	100 (16%)	74 (12%)	23 (4%)	68 (11%)

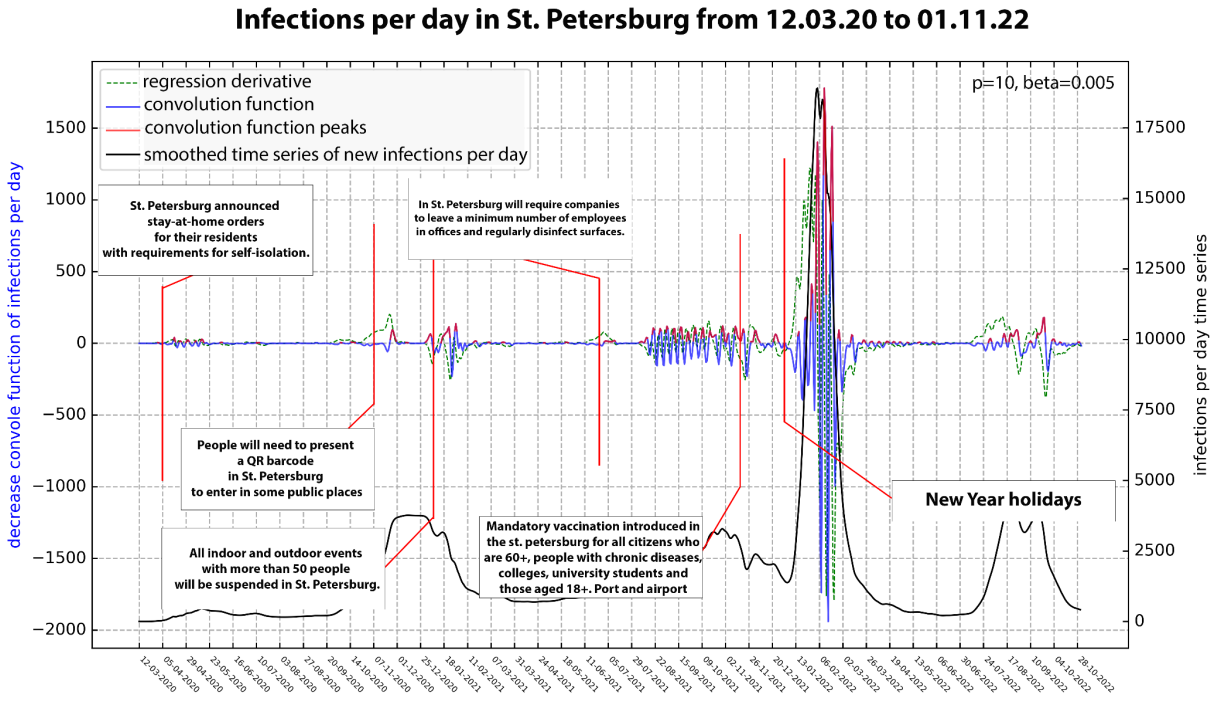

Figure 13: The smoothed time series graph of the number of new infections per day for St. Petersburg from 12.03.2020 to 01.11.2022 from YAND is shown in black; its convolution function graph and highlighted peaks by threshold α in blue and red, respectively. Red markers with textual explanations mark the dates of introduction of selected key restrictive measures.

class FF2 and increased control over the movement of people within the country.

Table 3 then presents for each study region the calculations of the percentage composition of recognized key restrictive measures, based on the WHO classification category. Based on the created table, a number of the following conclusions can be made:

1. most effective are measures aimed at limiting people's gatherings during their daily chores, such as going to places of work or higher education (WHO classification code 4.2) and public leisure activities (WHO classification code 4.3);

2. there are measures to restrict travel within the country (WHO code 4.5), cutting off coronavirus traffic from metropolitan areas to the periphery;

3. school-oriented measures (WHO code 4.1) are relatively small in comparison. This may be because children are more easily infected with coronavirus, making it more difficult to detect. However, we cannot rule out the fact that adolescents infected in educational institutions carry the infection home;

4. for St. Petersburg, more measures classified as restrictions in offices, enterprises and universities (code 4.2 according to the WHO classification) were recognized than for Moscow. However, in Moscow, more attention is paid to the protection of vulnerable groups (65+ years). In general, the recognized measures percentage per WHO database categories is similar for both regions, indicating an identical approach to hindering COVID-19 spread;

5. for the Republic of Austria, there is a relatively even percentage of categories according to the WHO classification.

3.3 Recognition of anomalous values of time series by FCARS algorithm

The time series of the number of new infections per day for the regions of the Russian Federation and the Republic of Austria that the authors adopted in the studies were analyzed for anomalies using the FCARS algorithm (Fuzzy Comparison Algorithm for Recognition of Signals) [*Gvishiani et al.*, 2003].

FCARS is one of the algorithms of DMA [*Agayan et al.*, 2018], a direction of data analysis based on the transfer of concepts of classical mathematical

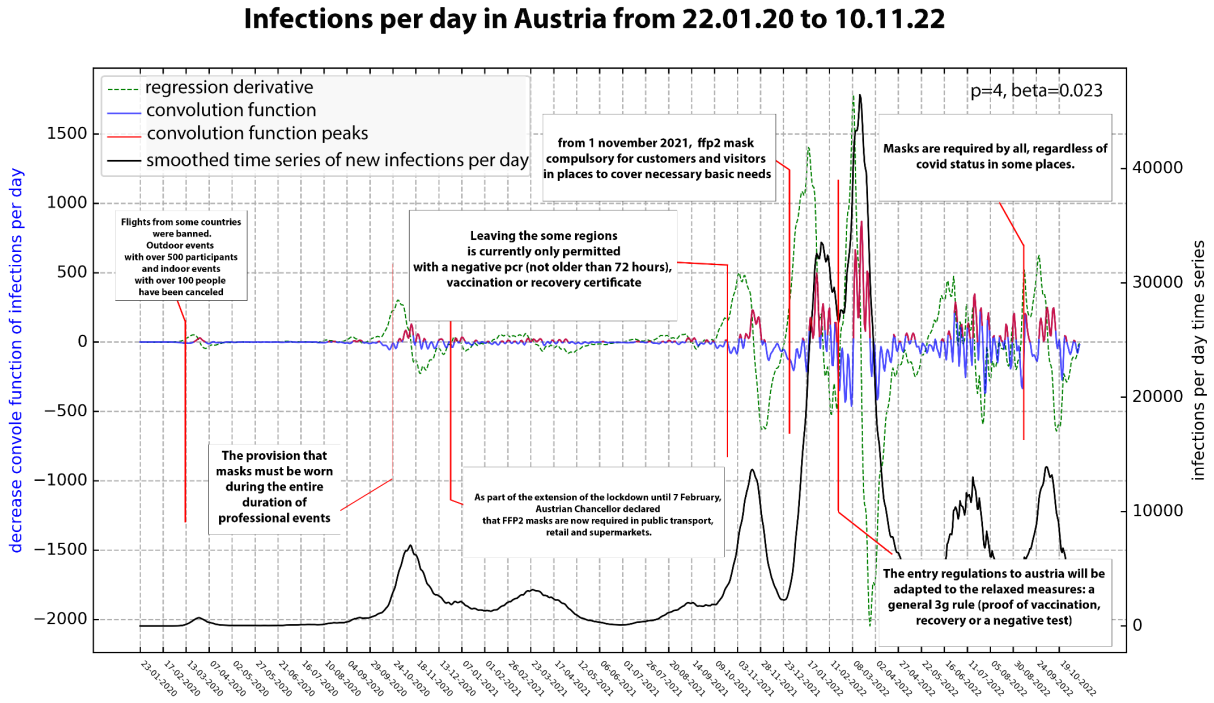

Figure 14: The smoothed time series graph of the number of new infections per day for Austria Rep. from 12.03.2020 to 10.11.2022 from JHU is shown in black; its convolution function graph and highlighted peaks by threshold α in blue and red, respectively. Red markers with textual explanations mark the dates of introduction of selected key restrictive measures.

analysis to the discrete case, developed for geophysical applications in the works of A. D. Gvishiani, S. M. Agayan, Sh. R. Bogoutdinov, B. A. Dzeboev, M. N. Dobrovolsky, and others. The results of applying FCARS to the time series of data on the number of new cases per day in the regions in question are shown in Figure 15–20.

It is clear from the figures that the FCARS algorithm identified areas of increased values of the number of new infections per day. Such areas correspond to the most severe phases of the epidemic. The application of the FCARS algorithm makes it possible to automatically determine the temporal boundaries of such severe phases using retrospective data. **When applied to newly reported data on the number of new infections per day can be used as a marker of the beginning of the next severe phase of a pandemic and the adoption of appropriate restrictive measures.**

4 Results interpretation

According to some claims in the media, COVID-19 morbidity is not such a serious cause of human mortality. However, when the authors compare the order of values of monthly mortality from road traffic accidents and COVID-19 in Moscow, one can see the multifold prevalence of mortality from the latter, as can be seen in Table 4.

The peaks of June 2021 observed in graphical visualizations of the number of new deaths per day series in Moscow (Figure 1c) and St. Petersburg (Figure 2c), as well as the steady growth of the total number of infected per date in Sevastopol (Figure 3d) and Crimea (Figure 4d), which began this month, correspond chronologically to the "delta" strain, characterized by high mortality [*Adjei et al.*, 2022].

The peaks at the turn of 2021 and 2022 observed in all subjects of the Russian Federation in graphical visualizations of the series of the number of new infections (Figure 1–5a) and cures (Figure 1–5b) chronologically correspond to the "omicron" strain, which is characterized by high morbidity and cure rates and low mortality, as confirmed by studies [*Adjei et al.*, 2022; *Sklyarov*, 2022].

Because of the strong positive correlation between the time series of new infections, recoveries and deaths per day for Moscow and St. Petersburg, a similar set of key restrictive measures can be observed in similar time ranges: introduction and control of self-isolation, closure of public eating places and restriction of the opening hours of recreational facilities. The weak correlation between the time series of the number of new infec-

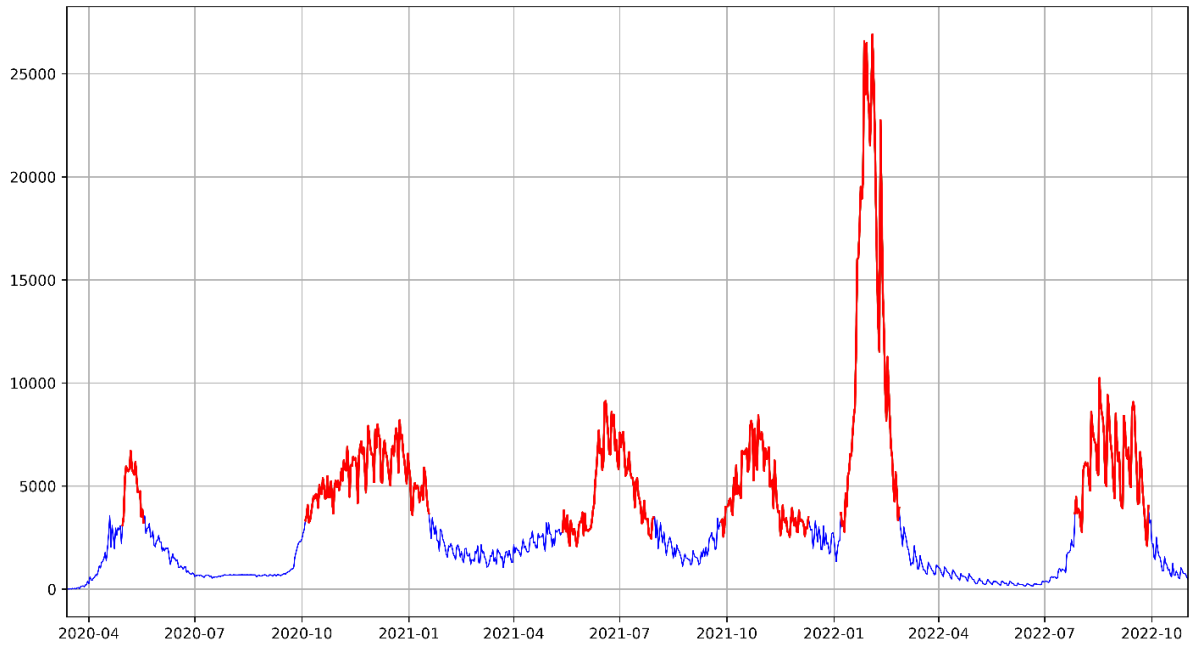

Figure 15: The time series graph of the number of new infections per day for Moscow from 12.03.2020 to 01.11.2022 from YAND is shown in blue; anomalies identified by the FCARS algorithm are shown in red.

Table 4: Monthly mortality from traffic accidents and COVID-19 in Moscow

Number of the month 2022 / deaths from:	1	2	3	4	5	6	7	8	9	10
COVID-19	2191	2314	1420	547	491	407	325	684	882	587
RTA	18	24	22	30	24	33	25	22	23	24

tions and deaths per day between any of the subjects of the Russian Federation and the Republic of Austria suggests that the course of the pandemic is different in the compared regions, so it does not make sense to look for a similar set of key restrictive measures.

By analyzing the recognized key restrictive measures identified by regression derivatives and their percentage composition based on WHO classification category affiliation, we can conclude that the decisive measures affecting the reduction of new infections per day from COVID-19 were limiting the number of people in public, workplace and intercity transport, identifying and isolating infections, and wearing personal protective equipment and hygiene measures.

By finding the intersection of the days obtained by regression derivatives and the FCARS algorithm, we can identify key restrictive measures that effectively influence the reduction of the number of new infections per day during the severe phases of the pandemic. For Moscow, the list of such measures is 91 out of 127 previously identified, for St. Petersburg it is 54 out of 61, and for the Republic of Austria it is 297 out of 630, respectively.

The method of regression derivatives and FCARS algorithm as components of DMA will be for the first time tested outside of geophysics problems. The algorithm is applied to time series of the number of new cases of COVID-19 infections per day for some regions of Russia and the Republic of Austria. This allowed to assess the nature and anomalies of pandemic spread as well as restrictive measures and decisions taken in terms of the administration of countries and territories.

Acknowledgements. This work was supported by the Russian Foundation for Basic Research project No. 20-57-82003 "System Analysis of patterns of COVID-19 spread in Europe and Russia", which is carried out jointly with the International Institute for Applied Systems Analysis (IIASA). The authors thank Dr. A. I. Rybkina for leading the project at the GC RAS in 2020-2022 and appreciate

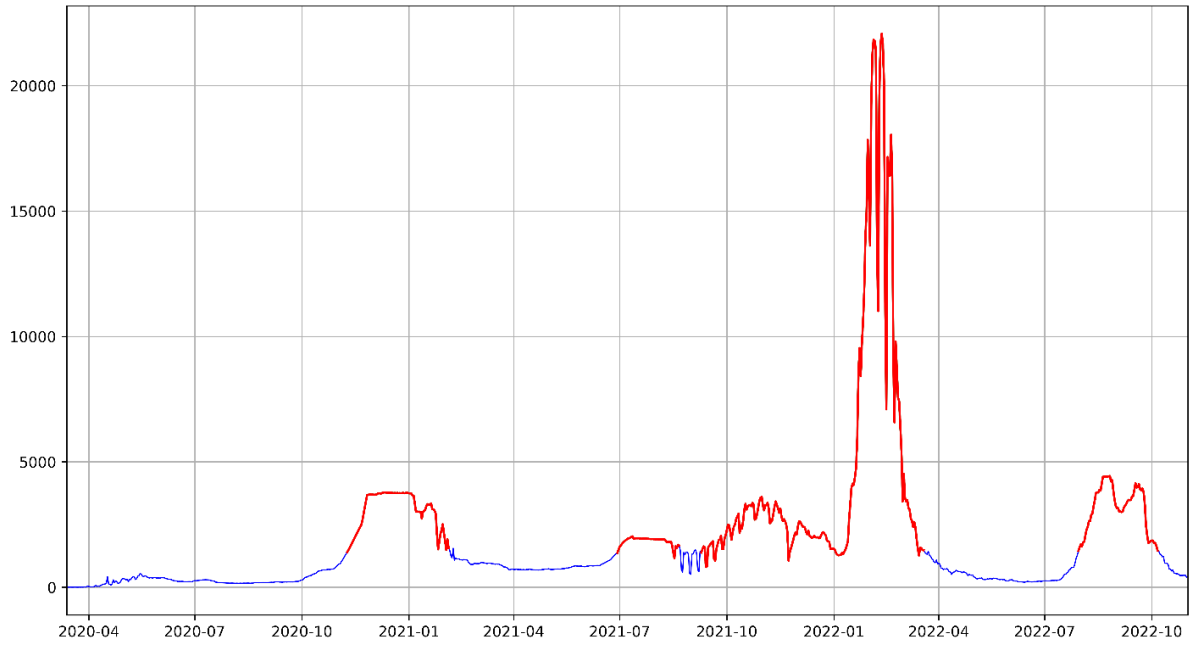

Figure 16: The time series graph of the number of new infections per day for St. Petersburg from 12.03.2020 to 01.11.2022 from YAND is shown in blue; anomalies identified by the FCARS algorithm are shown in red.

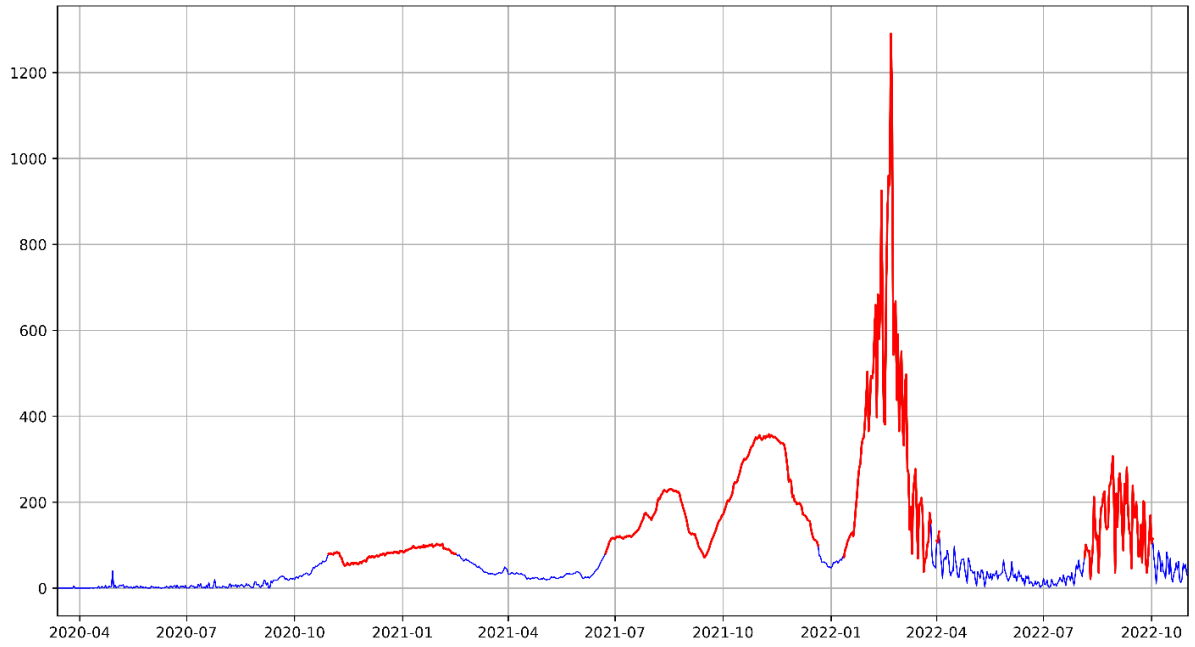

Figure 17: The time series graph of the number of new infections per day for Sevastopol from 12.03.2020 to 01.11.2022 from YAND is shown in blue; anomalies identified by the FCARS algorithm are shown in red.

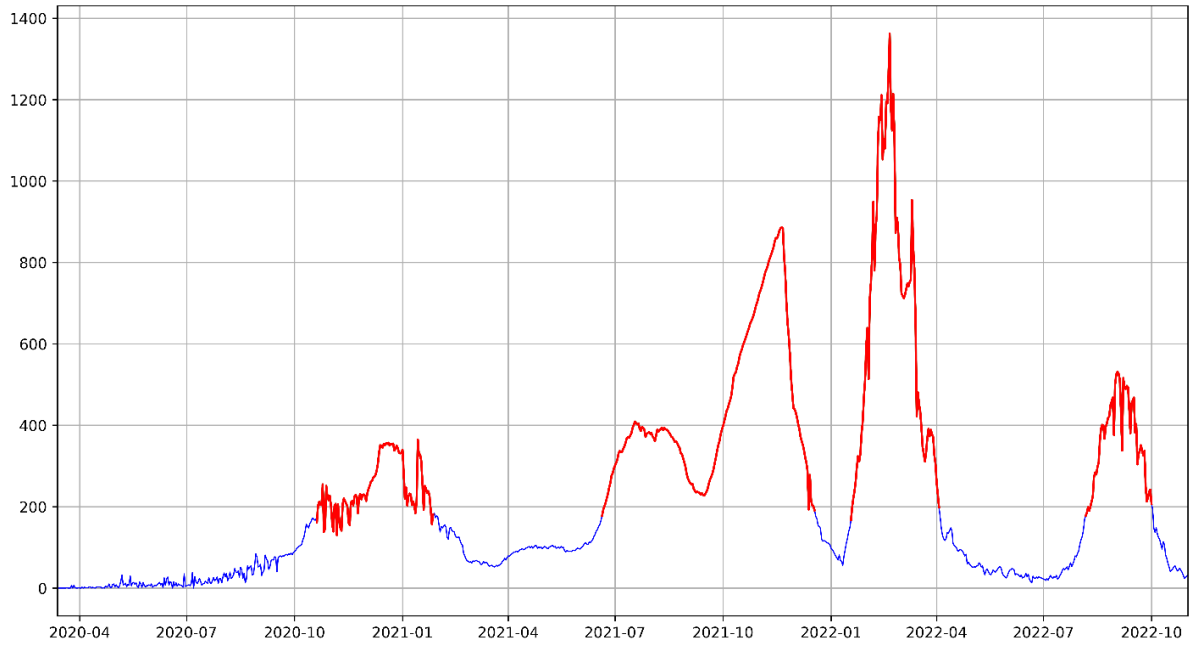

Figure 18: The time series graph of the number of new infections per day for Crimea Rep. from 12.03.2020 to 01.11.2022 from YAND is shown in blue; anomalies identified by the FCARS algorithm are shown in red.

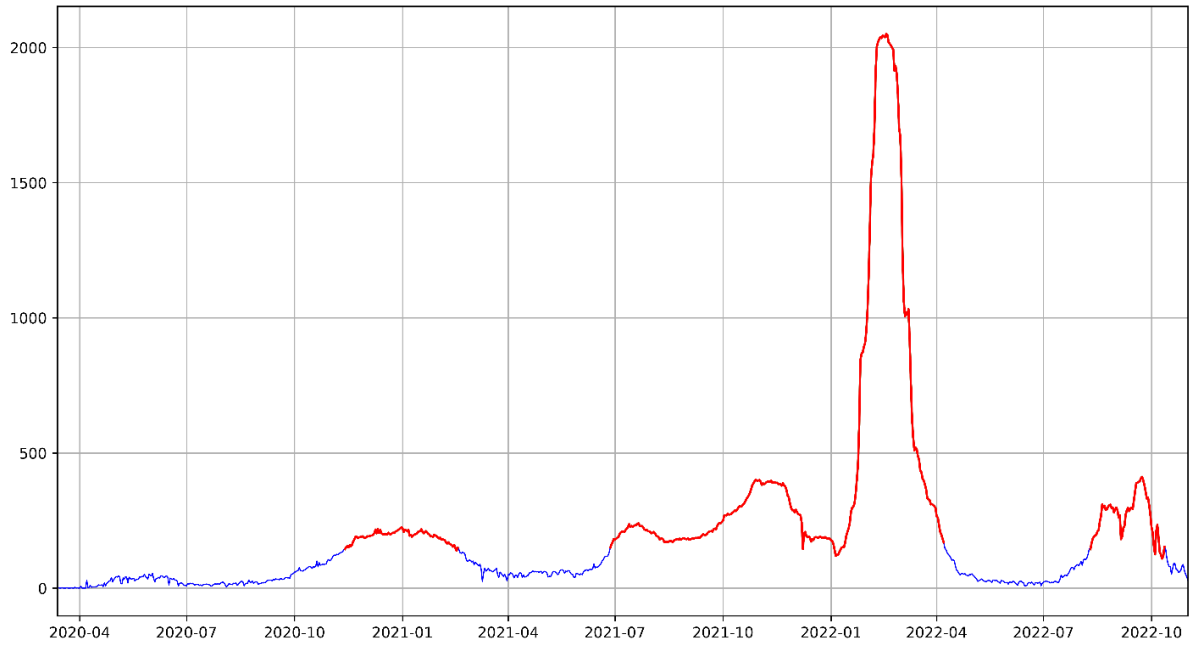

Figure 19: The time series graph of the number of new infections per day for Kaliningrad region from 12.03.2020 to 01.11.2022 from YAND is shown in blue; anomalies identified by the FCARS algorithm are shown in red.

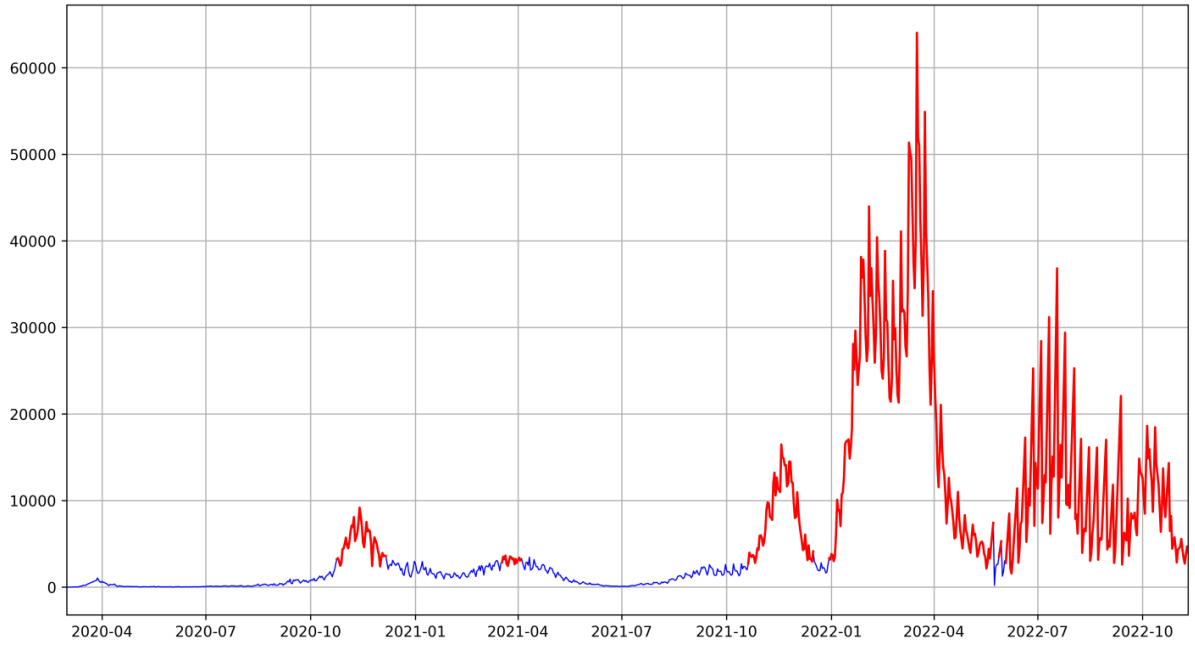

Figure 20: The time series graph of the number of new infections per day for Austria Rep. from 12.03.2020 to 01.11.2022 from JHU is shown in blue; anomalies identified by the FCARS algorithm are shown in red.

her important contributions during the first stages of the project.

References

Adjei, S., K. Hong, N.-A. M. Molinari, L. Bull-Otterson, U. A. Ajani, A. V. Gundlapalli, A. M. Harris, J. Hsu, S. S. Kadri, J. Starnes, K. Yeoman, and T. K. Boehmer (2022), Mortality Risk Among Patients Hospitalized Primarily for COVID-19 During the Omicron and Delta Variant Pandemic Periods - United States, April 2020 – June 2022, *MMWR. Morbidity and Mortality Weekly Report*, *71*(37), 1182–1189, doi:10.15585/mmwr.mm7137a4.

Agayan, S. M., Sh. R. Bogoutdinov, and R. I. Krasnoperov (2018), Short introduction into DMA, *Russian Journal of Earth Sciences*, *18*(2), ES2001, doi:10.2205/2018es000618.

Agayan, S. M., Sh. R. Bogoutdinov, D. A. Kamaev, and M. N. Dobrovolsky (2019a), Stochastic trends based on fuzzy mathematics, *Chebyshevskii Sbornik*, *20*(3), 92–106, doi:10.22405/2226-8383-2019-20-3-92-106, (in Russian).

Agayan, S. M., A. A. Soloviev, Sh. R. Bogoutdinov, and Yu. I. Nikolova (2019b), Regression derivatives and their application in the study of geomagnetic jerks, *Geomagnetism and Aeronomy*, *59*(3), 359–367, doi:10.1134/s0016793219030022.

Agayan, S. M., Sh. R. Bogoutdinov, M. N. Dobrovolsky, O. V. Ivanchenko, and D. A. Kamaev (2021), Regression differentiation and regression integration of finite series, *Chebyshevskii Sbornik*, *22*(2), 27–47, doi:10.22405/2226-8383-2021-22-2-27-47, (in Russian).

Aurambout, J.-P., C. Pettit, and H. Lewis (2008), Virtual Globes: the Next GIS?, in *Lecture Notes in Geoinformation and Cartography*, pp. 509–532, Springer Berlin Heidelberg, doi:10.1007/978-3-540-69168-6_25.

Dzeboev, B. A., A. A. Odintsova, A. I. Rybkina, and B. V. Dzeranov (2022), Assessment of the influence of astronomical cyclicity on sedimentation processes in the Eastern Paratethys based on paleomagnetic measurements using Discrete Mathematical Analysis, *Applied Sciences*, *12*(2), 580, doi:10.3390/app12020580.

GIBDD (2023), Information about the indicators of the state of road safety, http://stat.gibdd.ru/.

GitHub (2023), CSSEGISandData/COVID-19: Novel Coronavirus (COVID-19) Cases, provided by JHU CSSE, https://github.com/CSSEGISandData/COVID-19.

Gvishiani, A. D. (2019), Interdisciplinary Arctic Studies and System Analysis, in *V International Arctic Forum "Arctic: Territory of Dialogue" on 9–10 April*, St. Petersburg, Russia, (in Russian).

Gvishiani, A. D., S. M. Agayan, Sh. R. Bogoutdinov, A. V. Ledenev, Z. Zlotniki, and Z. Bonnin (2003), Mathematical Methods of Geoinformatics. II. Fuzzy-Logic Algorithms in the Problems of Abnormality Separation in Time Series, *Cybernetics and Systems Analysis*, *39*(4), 555–563, doi:10.1023/b:casa.0000003505.56410.4f.

Gvishiani, A. D., S. M. Agayan, and Sh. R. Bogoutdinov (2008), Fuzzy recognition of anomalies in

time series, *Doklady Earth Sciences*, *421*(1), 838–842, doi:10.1134/s1028334x08050292.

Huang, C., Y. Wang, X. Li, et al. (2020), Clinical features of patients infected with 2019 novel coronavirus in Wuhan, China, *The Lancet*, *395*(10223), 497–506, doi:10.1016/s0140-6736(20)30183-5.

Kolmogorov, A. N., and S. V. Fomin (2004), *Elements of the Theory of Functions and Functional Analysis*, 7th ed., Fizmatlit, Moscow, (in Russian).

Odintsova, A., A. Rybkina, J. Nikolova, and A. Korolkova (2020), GIS Project ROSA: FAIR Principles in the Petroleum Industry, *Data Science Journal*, *19*(1), 13, doi:10.5334/dsj-2020-013.

ORBUS Web (2019), http://data.sph.gcras.ru/OrbusWeb.html?/COVID-19.

Rospotrebnadzor (2023), Answers to frequently asked questions about coronavirus infection COVID-19, http://86.rospotrebnadzor.ru/territorialnye-otdely/ug/otvety-na-chasto-zadavaemye-voprosy-po-koronavirusnoj-infekcii-covid-19.

Rossiyskaya Gazeta (2022), Preliminary results of the All-Russian Population Census, https://rg.ru/2022/05/30/predvaritelnye-itogi-vserossijskoj-perepisi-naseleniia.html.

Saxena, R., M. Jadeja, and V. Bhateja (2022), *Exploring Susceptible-Infectious-Recovered (SIR) Model for COVID-19 Investigation*, 53 pp., Springer Nature Singapore, doi:10.1007/978-981-19-4175-7.

Sklyarov, B. A. (2022), Research data and conclusions pertaining to the omicron strain of coronavirus (COVID-19), *International Journal of Humanities and Natural Sciences*, pp. 102–105, doi:10.24412/2500-1000-2022-5-1-102-105, (in Russian).

Soloviev, A. A., A. I. Gorshkov, and A. A. Soloviev (2016), Application of the data on the lithospheric magnetic anomalies in the problem of recognizing the earthquake prone areas, *Izvestiya*, *Physics of the Solid Earth*, *52*(6), 803–809, doi:10.1134/s1069351316050141.

World Health Organization (2019), Public Health and Social Measures, https://www.who.int/emergencies/diseases/novel-coronavirus-2019/phsm.

Yandex DataLens (2023), Coronavirus. Dashboard and data.